Environmental Science
Processes & Impacts

Accepted Manuscript

ROYAL SOCIETY OF CHEMISTRY

rsc.li/process-impacts

Volatilization of elemental mercury from fresh blast furnace sludge mixed with basic oxygen furnace sludge under different temperatures

Corinna Földi[1], Reiner Dohrmann[2], and Tim Mansfeldt[1]*

[1] Department of Geosciences, Soil Geography/Soil Science, University of Cologne, D-50923 Köln, Germany

[2] Bundesanstalt für Geowissenschaften und Rohstoffe (BGR)/Landesamt für Bergbau, Energie und Geologie (LBEG), Stilleweg 2, D-30655 Hannover, Germany

* Corresponding author

Phone: ++49-(0)221470-7806

Fax: ++49-(0)221470-5124

Email: tim.mansfeldt@uni-koeln.de

Abstract

Blast furnace sludge (BFS) is a waste with elevated mercury (Hg) content due to enrichment during the production process of pig iron. To investigate the volatilization potential of Hg, fresh samples of BFS mixed with basic oxygen furnace sludge (BOFS; a residue of gas purification from steel making, processed simultaneously in the cleaning devices of BFS and hence mixed with BFS) were studied in sealed column experiments at different temperatures (15, 25, and 35 °C) for four weeks (total Hg: 0.178 mg kg^{-1}). The systems were regularly flushed with ambient air (every 24 h for the first 100 h, followed by every 72 h) for 20 min at a flow rate of 0.25 ± 0.03 L min^{-1} and elemental Hg vapor was trapped on gold coated sand. Volatilization was 0.276 ± 0.065 ng ($\bar{x}_m$: 0.284 ng) at 15 °C, 5.55 ± 2.83 ng ($\bar{x}_m$: 5.09 ng) at 25 °C, and 2.37 ± 0.514 ng ($\bar{x}_m$: 2.34 ng) at 35 °C. Surprisingly, Hg fluxes were lower at 35 than 25 °C. For all temperature variants, an elevated Hg flux was observed within the first 100 h followed by a decrease of volatilization thereafter. However, the background level of ambient air was not achieved at the end of the experiments indicating that BFS mixed with BOFS still possessed Hg volatilization potential.

Keywords: Blast furnace sludge, Basic oxygen furnace sludge, Mercury, Steel making sludge, Volatilization

1. Introduction

Blast furnace sludge (BFS) and basic oxygen furnace sludge (BOFS) are typical steelmaking-related wastes. Both are generated during the wet purification process of effluent gases. While BFS occurs in the cleaning of blast furnace top gas, BOFS is a residue of gas purification from steel making in so-called basic oxygen furnaces, more popularly known as Linz-Donauwitz (LD) converters. The latter converts molten pig iron into low carbon steel via lancing pure oxygen (O_2) in a mixture of pig iron, iron (Fe) scrap, ferroalloys, lime, and Fe ores. During the blowing process, large amounts of fumes and gases are generated containing fine particles of the charge materials. Pig iron is produced in blast furnaces by transferring Fe from ores into its elemental form. Thereby, charge material, such as Fe ores, high carbon (C) fuels (e.g. coke), and flux additives, are smelted in the blast furnace at temperatures up to 2200 °C. During the combustion process, the blast furnace gas drags along solid phases of the charge material and their reaction products. Both effluent gases are progressively cleaned in, for example, axial cyclones or dust-catchers to separate out coarse particles, while fine particles are removed using electrostatic precipitators or annular gap scrubbers. After the separation of solid material from the bulk of the process water, the resulting muddy waste is referred to as BFS and BOFS, respectively.

To reduce financial expense for virgin raw material and depositing costs, the integrated steel-making industry has put in a lot of effort to find ways of utilizing its byproducts, especially as many of the byproducts still contain high amounts of the demanded C and Fe compounds. However, due to the high temperatures in both processes, low melting point elements, such as lead (Pb), potassium (K), sodium (Na), and zinc (Zn) are partially vaporized. In the effluent gas, they are either present in their gaseous phase or associated with fine particles. Hence, these elements are accumulated and enriched in BFS and BOFS, respectively.[1-6] These elements among

others (sulfur (S), cadmium (Cd), and cyanides) inhibit the utilization of BFS and BOFS in the integrated steel industry as they can cause operational difficulties in the blast furnace.[5] Also, the rather fine grain size character of this waste hinders the internal recycling as feed for the sintering process.[7]

The accurate amount of sludge per Mg of pig iron varies from plant to plant. However, based on an annual worldwide production of 1.168 10^6 Mg of pig iron[8] and the stated 6 kg of BFS per Mg of pig iron[9] approximately 7 10^6 Mg of BFS are generated each year. As 70 % of the annual crude steel production of 1.600 10^6 Mg[10] are produced via the basic oxygen furnace process with an estimated 17.0 to 22.8 kg of BOFS per Mg of crude steel[11], roughly 31 10^6 Mg of BOFS are generated globally per year.

Consequently, large amounts of this industrial waste need to be deposited. Despite their toxic properties, BFS and BOFS have long been deposited in large surface landfills in industrial areas in Europe, which still might be an ongoing procedure in countries with less strict environmental laws.

In our previous study[12], we proved the enrichment of the volatile element Hg in BFS with contents ranging from 0.006 up to 20.8 mg kg^{-1} (median ($\tilde{x}_m$): 1.64 mg kg^{-1}; mean ($\bar{x}_a$): 3.08 mg kg^{-1}). Mercury is considered to be one of the most important environmental pollutants, as the element and many of its compounds are highly toxic, persistent, and readily released into the environment due to their high mobility and volatility.[13] Anthropogenic activities have led to a significant increase in Hg concentration in all environmental compartments.[14] Besides anthropogenic release, re-emission of “natural and anthropogenic” Hg from the Earth’s surface contributes significantly to the global Hg cycle (approximately 60 %).[14] Whereas re-emissions from oceans have undergone recent scientific interest, little is known about the amounts, species, and the factors causing Hg volatilization from the land’s surface.

Although oxidized Hg (Hg^{2+}) is the predominant form of Hg in soils, it is widely accepted that Hg volatilizing from soils is predominantly in the form of elemental Hg (Hg^0) and/or dimethyl Hg, probably with minor amounts of monomethyl Hg and soluble Hg(II)-salts.[15] The former are the only Hg species described as volatile species as they are water soluble with at least 500 times higher air/water-distribution constant than the non-volatile species.[16] Formation and turnover of Hg^{2+} to Hg^0 in soils is controlled by both biotic and abiotic reduction.[15] While abiotic reduction is basically mediated by humic acids, fulvic acids, and other reductants, such as Fe^{2+}, biotic reduction is capable through Hg resistant soil microorganisms.

Several key factors besides total Hg content and speciation were identified as influencing Hg degassing from soils. Besides solar radiation, temperature, and elevated soil moisture, interactions with atmospheric ozone and turbulences significantly affect Hg fluxes. Previous work showed that Hg emissions from soils correlate positively with ambient air temperature, soil surface temperature, and solar radiation, while they are negatively correlated with relative humidity and soil wetness.[17] As soil surface temperature is basically a result of ambient air temperature and solar radiation, both these factors are the main key factors driving Hg emissions at a given Hg content.

Even less is known about Hg emissions from industrial wastes and their disposal sites, respectively. Few publications deal with Hg fluxes from municipal solid waste landfill sources, emphasizing the importance for the global Hg cycles.[18-20] Mercury in the atmosphere exists predominantly as elemental (Hg^0), oxidized (Hg^{2+}), and particulate (Hg_p) Hg with Hg^0 typically making up more than 98 % of total gaseous Hg.[21] We henceforth use Hg to refer to elemental Hg vapor.

However, to our knowledge, no data has been published about the degassing of Hg from metallurgical wastes such as BFS or BOFS. In this study, our objectives were (i)

to study if any Hg is degassed from the described wastes, (ii) to quantify the amount of volatizing Hg, and (iii) to determine the effect of temperature on the Hg flux by excluding other known parameters affecting Hg degassing.

2. Material and methods

2.1. Sampling site, sampling, and sample preparation

One sample of BFS mixed with BOFS, henceforth referred to as BFS/BOFS, was taken from after the settling tank as the integrated steel plant in Germany, to be most cost effective, uses a joint cleaning process for both effluent gases. Unfortunately, pure BFS was not available. The sample was transferred into 10-litre buckets made of high-density polyethylene (HDPE) and homogenized. The buckets were completely filled, sealed with Teflon tape, directly transported to the laboratory, and stored in the refrigerator (4 °C) until used. The buckets, as all other equipment used in the column experiments, were previously washed with detergent, soaked several days with 10 % nitric acid (HNO_3), and rinsed with milli-Q Millipore water. A subsample was dried at room temperature and ground to analytical grain size in a mixer mill (MM400, Retsch) with zirconium oxide grinding tools.

2.2. Material characterization

2.2.1. Elemental composition

Total C, nitrogen (N), and sulfur (S) were quantified by dry combustion with an elemental analyzer (Vario EL Cube CNS, Elementar). The evolved gases carbon dioxide (CO_2), sulfur dioxide (SO_2), and nitrogen (N_2) were measured by thermal conductivity. Total carbonate-carbon (TCC) was determined by the suspension method using a DIMATOC® 100 liquid analyzer (Dimatec Corp.) Total residual C

(TRC) was calculated from the difference between total C and TCC. Residual C contains C in the form of coke, graphite, and black C.

Other elements were analyzed by wavelength dispersive X-ray fluorescence (XRF; Axios, PANalytical). Powdered samples were mixed with a flux material and melted into glass beads. To determine loss on ignition (LOI), 1.0 g of sample material was heated to 1030 °C for 10 min. After mixing the residue with 5.0 g of lithium metaborate ($Li_2B_4O_7$) and 25 mg of lithium bromide (LiBr), it was fused at 1200 °C for 20 min. The calibrations were validated regularly by analysis of the reference materials and 130 certified reference materials were used for the correction procedures.

Total Hg was analyzed by means of a direct Hg analyzer (DMA-80, MLS GmbH). The sample was thermally decomposed at 750 °C in a continuous flow of analytical grade O_2 and, hence, combustion products were carried off through a catalyst furnace where chemical interferences were removed. The Hg vapor was trapped on a gold amalgamator and subsequently desorbed for spectrophotometric determination at 254 nm. The instrument was calibrated with 7 levels of concentrations for each “absorbance cell” of the detector (low concentration “absorbance cell” ranged up to 2 ng, higher concentration “absorbance cell” ranged from 2 to 22 ng). Mercury solutions for calibration were prepared by serial dilution from 1000 ± 2 mg L^{-1} Hg standard solution (CertiPur Merck, traceable to SRM from NIST) in 2 mM BrCl. The coefficient of determination was 0.9989 for the low concentration “absorbance cell” and 0.9999 for higher concentration “absorbance cell”. The instrument did not have to be recalibrated every day as no significant instrumental parameter had to be replaced. In every-day operation, analytical quality was assured by measuring the same liquid standards as used for the calibration prior, during and after sample analyses. The amount of detected Hg in the standards was chosen for the range of

experimental values (0.1 ng (σ_{rel} = 9.1 %), n = 108; 1 ng (σ_{rel} = 3.75 %), n = 54; and 10 ng (σ_{rel} = 4.16 %), n = 36).

2.2.2 Mineralogical composition

X-ray powder diffraction (XRD) patterns were recorded using X-ray diffraction (X'Pert PRO MPD theta–theta, PANalytical) with Co-Kα radiation generated at 40 kV and 40 mA. The device was equipped with a variable divergence slit (20 mm irradiated length), primary and secondary sollers, diffracted beam monochromator, a point detector, and a sample changer (sample diameter 28 mm). The samples were investigated from 1° to 80° 2Θ with a step size of 0.03° 2Θ and a measuring time of 10 s per step.

For specimen preparation, the back-loading technique was used. Phase identification was made by reference to patterns in the International Center for Diffraction Data (ICDD) PDF-2 database, released in 2009.

2.3. Column experiments

To study the gaseous release of elemental Hg under different temperatures, column experiments were conducted. The column installation consisted of a borosilicate glass flux chamber with one outlet and four inlets according to Ringklebe et al.[22], a PVC cylinder with a height of 6 cm and a diameter of 11.5 cm, a column frame to seal the column base, and a gas sampler (GS 212, Desaga) (Fig. 1). Aliquots of BFS/BOFS (500 to 800 g fresh material) were transferred into the columns in four replicates; the flux chambers were fixed on the cylinders, and sealed tightly using Teflon tape. Re-homogenization was not carried out before sampling for each temperature variant to avoid further contact with O_2. The column installations were placed in an incubator (KB 400, Binder) at 15, 25, and 35 °C for 28 days. Inlets and

outlets, respectively, of the flux chamber were sealed with blind plugs made of borosilicate glass. Experiments were conducted in the dark to exclude solar radiation and hence possible photocatalytic reduction of soluble Hg^{2+} to volatile Hg^0 at the surface. The lowest temperature variant was chosen to be 15 °C as it is the annually-averaged temperature across global land and ocean surfaces for 2014 (14.59 °C) .[23] However, as the BFS/BOFS was black, it exhibits a rather lower albedo (< 15 %) and hence the surface can easily be warmed at temperatures higher than the ambient air. That is why we chose temperature variants of 25 and 35 °C.

To determine Hg volatilization, four gold traps were connected in line directly to the flux chamber's outlet. The gold traps were heated at 110 °C using a heating band (HS, Horst GmbH) and thermostat (HT22, Horst GmbH) to avoid water re-condensing. To close the circulation, the gold traps were further connected to the gas sampler and tubing lines were connected between the gas sampler and the four inlets of the flux chamber using borosilicate glass, Tygon, and Teflon tubings, respectively. Ambient air was pumped through the closed circulation system using the gas sampler for 20 min at 0.25 ± 0.03 L min^{-1}, as these parameters had been shown to be the most effective in preliminary experiments. Sampling was undertaken after 24, 48, 72, 96, and then every 72 h resulting in 12 sampling events. Blanks of ambient air were taken at the beginning of the experiment by connecting four gold traps to the gas sampler and sucking air through the traps for 20 min with a flow rate of 0.25 L min^{-1}. Sampling blanks were found to be 0.0433 ng on average. This value was subtracted from the quantities of Hg collected on the traps during the experiments.

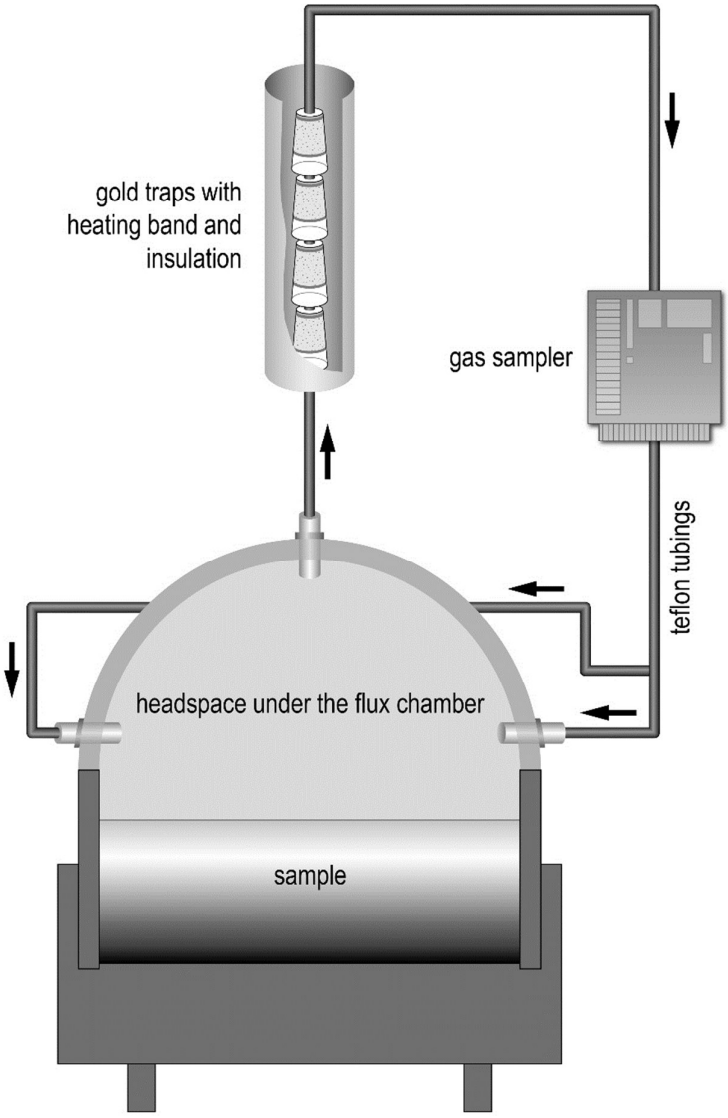

Fig. 1: Scheme of experimental design for sampling elemental Hg

To reduce the Hg capacity of the gold coated sand (GCSI; Timmerman gold trap, Symalab) to an effective measuring range of the DMA-80, GCSI was mixed with quartz powder (pro analysis, Merck) with a weight-to-weight ratio of 1 to 50, referred to as GCSII hereafter. Gold traps consisted of borosilicate glass tubings filled with 1 g GCSII and fixed with quartz wool. Each gold trap was stored in a separate borosilicate vessel with a Teflon-lined cap and was measured within 3 days using the

DMA-80. Three procedural standards were processed with the column and analyzed with known amounts of 1, 10, and 100 g Hg resulting in recoveries of 80.6, 64.3, and 73.3 %, respectively.

Water content at the beginning and the end of each experiment was calculated by mass using the following formula:

$$water\ content\ [\%] = \frac{mass\ (a) - mass\ (b)}{mass\ (a)} * 100$$

water content$_{start}$: a = mass$_{start}$; b = mass$_{105\ °C}$

water content$_{end}$: a = mass$_{end}$; b = mass$_{105\ °C}$

For mass at 105 °C, the residue of each column was dried for one week at room temperature; a subsample of each column was weighed (15 g) and dried for 24 h at 105 °C. Further, the factor of each subsample at 105 °C to the mass of each column at room temperature (start and end, respectively) was calculated and considered for the water content.

All measured Hg values were calculated on a dry mass basis (mass$_{105\ °C}$) to ensure an accurate comparison.

3. Results and discussions

3.1. Material characterization

3.1.1. Elemental composition

The elemental composition of BFS and BOFS differed significantly due to the applied raw materials and byproducts.[2-4, 12, 24, 25] The composition of the analyzed sample was clearly dominated by C (60.6 g kg^{-1}) and Fe (564 g kg^{-1}) reflecting the metallurgical production process (Table 1). The higher proportion of Fe was typical for BOFS as it is known that it may contain from about 50 to as much as 75 % Fe.[4] In fact, since two-thirds of the sludge was made up of Fe it might be a potential raw

material to be recycled in the sintering process. High Fe content indicated a dominance of BOFS in the studied sample as Fe content in BFS mainly ranged from around 100 to 300 g kg^{-1}.[2, 12, 24, 25] In addition, the rather low C content of the sample underlined this, as C in BFS normally ranged between an average of 160 and 190 g kg^{-1}.[2, 12, 25] However, TCC in respect to total C was 16.8 %, in the same range as BFS.

The chromium (Cr), titanium (Ti), copper (Cu), and nickel (Ni) contents ranged from 665 to 207 mg kg^{-1} and were considered to be low. However, the Zn content of 14.8 g kg^{-1} was significantly higher being rather in the range stated for BOFS[3] than for BFS.[2, 12, 24, 26] As stated by Makkonen et al.[6] the Zn content in BOFS was generally around 2 mass-% but could be increased to 25 mass-% if scrap was recycled in the converter. Consequently, the Zn content of the sample in this study suggested a rather low recycling fraction of scrap. Moreover, the elevated Zn value most likely inhibited direct recycling of this material to the sintering process as was suggested before. The Zn content entering the blast furnaces should not exceed 120 g Zn per Mg of pig iron as its compounds may form solids on the furnace walls, which in turn cause operational difficulties in the blast furnace operation.[26] The maximum loading would be reached with only 8 kg of the material under study. Common loadings of Fe-making blast furnaces range between 576 and 1320 kg of sinter and 351 and 734 kg of pellets per Mg of pig iron.[27] As a consequence, BFS/BOFS needed either to be used as landfill or further processed to reduce the Zn content. The processing of steelmaking dust, such as electric arc furnace dust, by hydrometallurgical or pyrometallurgical methods has attracted recent scientific interest. However, for BFS and BOFS further processing is far more complicated due to the relatively low Zn content compared with electric arc furnace dust.[3]

Table 1: Chemical composition of blast furnace sludge mixed with basic oxygen furnace sludge

element	unit	value
C	g kg^{-1}	60.6
TCC[a]		10.2
TRC[b]		50.4
S		2.34
Fe		564
O		280
Ca		45.2
Zn		14.8
Si		10.6
Mn		9.12
Al		2.65
Mg		2.29
Pb		1.06
Cr	mg kg^{-1}	665
P		524
Ti		444
K		340
Cu		286
Ni		207
Hg		0.178
Na		<0.01
LOI[c]	[%]	5.70

[a] Total carbonate-carbon [b] Total residual carbon [c] Loss on ignition

The total Hg content of the sample was 178 ± 3.26 µg kg^{-1} (n = 4). In our previous study the Hg content of 65 dumped BFS samples from seven locations varied between 0.006 up to 20.8 mg kg^{-1} with a ($\overline{x}_m$) of 1.64 mg kg^{-1} ($\overline{x}_a$: 3.08 mg kg^{-1}). Consequently, the analyzed sample was rather low in Hg content, which most likely resulted from the addition of the BOFS to the BFS during the cleaning process. In

fact, soils with a similar Hg content (between 0.15 and 0.2 mg kg^{-1}) would be regarded as reflecting the natural background content of Hg.[28]

3.1.2 Mineralogical composition

The phase composition of BFS/BOFS (Fig. 2) revealed the presence of different Fe phases, such as magnetite (Fe_3O_4), wüstite (FeO), hematite (Fe_2O_3), and α-Fe. Furthermore, quartz (SiO_2), calcite ($CaCO_3$), and perovskite ($CaTiO_3$) were detected by XRD. Other phases, as indicated by the chemical composition, could not be clearly identified either as a result of their minor amounts and/or their vanishing in the background of the XRD pattern. Despite the elevated Zn content of 14.8 g kg^{-1}, no Zn-bearing phase was detected. Trung et al.[3] summarized several approaches for the lack of identified Zn phases. According to these authors, Zn might be distributed in various phases such as zincite (ZnO), franklinite ($ZnFe^{III}O_4$), and solid solutions of franklinite and hence their diffraction could vanish into the background of the pattern. Furthermore, they pointed out that amorphous fractions as well as present C increased the background signal, intensifying the vanishing of certain peaks. However, Kretzschmar et al.[24] identified five major types of Zn in BFS using a combination of synchrotron XRD, micro-XRF, and X-ray adsorption spectroscopy at the Zn K-edge for solid phase. These were (i) Zn in the octahedral sheets of phyllosilicates, (ii) Zn sulfide minerals (ZnS, sphalerite, or wurtzite), (iii) Zn in a KZn−ferrocyanide phase ($K_2Zn_3[Fe(CN)_6]_2 \cdot 9H_2O$), (iv) hydrozincite ($Zn_5(OH)_6(CO_3)_2$), and (v) tetrahedrally coordinated adsorbed Zn occurring in variable amounts. Zincite was detected only in traces, while $ZnFe^{III}O_4$ was not detected at all. Another approach explained the lack of Zn phases by the isomorphic structures of identified ferrites and the resulting difficulties in distinguishing the diffraction peaks, e.g. Fe_3O_4 and $ZnFe^{III}{}_2O_4$. In addition, the structural substitution of Fe by Zn in Fe_3O_4 is

reasonable. The increasing baseline between 30 and 45 °2Θ in this pattern indicated the significant presence of X-ray amorphous phases underlying this statement. Various authors have shown the presence of significant amounts of XRD amorphous phases in BFS, mainly being coke- and graphite-bound C.[2, 24, 29]

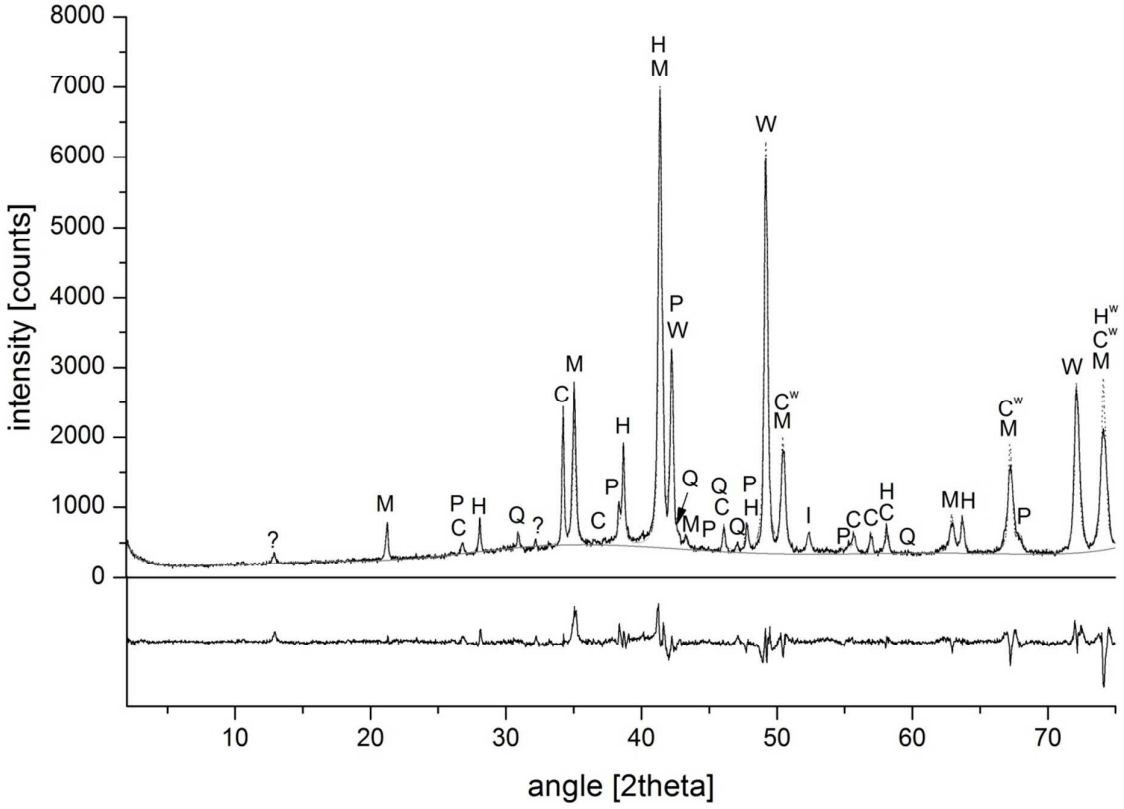

Fig. 2: Powder X-ray diffraction (XRD) pattern of a mixture of blast furnace sludge and basic oxygen furnace sludge. The black line represents the experimental XRD pattern, the dotted black line the calculated Rietveld pattern, and the baseline is given as the approximately horizontal line below (light grey). C: calcite; H: hematite; I: α-Fe; M: magnetite; P: perovskite; Q: quartz; W: wüstite; ^{w}: weak signal

3.2. Column experiments

The water content of the columns was 53.1 ± 1.5 % (Table 2; $\bar{x}_m$: 53.7 %; n = 4) for 15 °C, 51.4 ± 1.0 % ($\bar{x}_m$: 51.4 %; n = 4) for 25 °C, and 44.6 ± 3.2 % ($\bar{x}_m$: 43.6 %; n =

4) for 35 °C at the beginning of the experiment as a suspension was formed during storage. For all temperature ranges, the columns were not fully dewatered due to the limited headspace and resulting water vapor pressure. However, water content of the columns after four weeks was 47.4 ± 0.8 % ($\overline{x}_m$: 47.5 %; n = 4) for 15 °C, 46.7 ± 1.7 % ($\overline{x}_m$: 46.9 %; n = 4) for 25 °C, and 39.0 ± 3.0 % ($\overline{x}_m$: 37.9 %n = 4) for 35 °C. This represented a decrease of 5.7 ± 1.0 % ($\overline{x}_m$: 5.7 %; n = 4) for 15 °C, 4.7 ± 1.2 % ($\overline{x}_m$: 4.8 %; n = 4) for 25 °C, and 5.6 ± 1.1 % ($\overline{x}_m$: 5.5 %; n = 4) for 35 °C. As the samples were not re-homogenized before each individual experiment variant, higher bulk density and hence lower water content are reasonable for the later experiments.

Figure 3 shows the averaged vapor phase Hg release from the columns at different temperatures. Within the first 100 h, daily Hg flux was 0.297 ± 0.077 ng ($\overline{x}_m$: 0.301 ng) for the 15 °C temperature variant. Afterwards, trapped Hg release was 0.266 ± 0.061 ng ($\overline{x}_m$: 0.284 ng). However, the sampling period after the first 100 h was on 72 h instead of daily bases. Consequently, volatilization was elevated during the first days and decreased slightly thereafter. In total, less than 0.001 % of total Hg of the BFS/BOFS degassed within 4 weeks. The background level of ambient air (0.0433 ± 0.0035 ng per 5.2 L), however, was not achieved at the end of the experiment, indicating that BFS/BOFS still possessed the potential for Hg volatilization after storage at 15 °C. To exclude Hg saturation in the headspace and hence reduced Hg volatilization, saturation concentration of Hg at 15 °C was calculated using data from the Occupational Safety & Health Administration[30] and was approximately 9 µg L^{-1}. With respect to the headspace volume of 0.65 L, this would result in a max. Hg release of approximately 6,000 ng, being far higher than the actual measured values. Besides, reduced air pressure was avoided by using headspaces with air circulation systems as described by Rinklebe et al..[22] The

continuous gas movement over the sample's surface virtually eliminated reduced air pressure.

Table 2: Weight and water content specification of the columns and the temperature variants

		column I	column II	column III	column IV
15 °C	$mass_{start}$	750	688	799	858
	$mass_{end}$	653	610	717	785
	$mass_{105\ °C}$	347	318	377	425
	water $content_{start}$ [%]	54.2	54.1	53.3	51.0
	water $content_{end}$ [%]	47.2	48.2	47.8	46.3
25 °C	$mass_{start}$	665	553	515	530
	$mass_{end}$	613	519	460	479
	$mass_{105\ °C}$	319	273	251	268
	water $content_{start}$ [%]	52.6	51.1	51.8	50.2
	water $content_{end}$ [%]	48.4	47.9	45.9	44.7
35 °C	$mass_{start}$	582	604	584	611
	$mass_{end}$	519	554	543	550
	$mass_{105\ °C}$	330	344	342	313
	water $content_{start}$ [%]	43.7	43.5	42.0	49.2
	water $content_{end}$ [%]	36.7	38.3	37.6	43.4

The saturation concentration for 25 °C (20 µg L^{-1}, which corresponds to about 15 µg Hg release to the headspace volume of 0.65 L) was also higher than the measured Hg values: Hg fluxes was 8.45 ± 3.01 ng ($\bar{x}_m$: 7.23 ng) per day within the first 100 h and decreased from 6.20 to 2.82 ng per 72 h thereafter (4.10 ± 1.24 ng; $\bar{x}_m$: 3.48 ng), resulting in volatilization of 0.25 % of the total Hg. Hindersmann et al.[31] analyzed Hg volatilization from undisturbed floodplain soil samples with a total Hg content of 9.2 ± 0.2 mg kg^{-1} at 20 °C using similar column installations. Mercury flux ranged between 0.4 ng and 411 ng per 72 h. Hence, Hg volatilization from BFS/BOFS can be described as rather low for this temperature range. It is known that two predominant factors control emissions from Hg-enriched soils, being soil Hg content and incident radiation.[32] Most likely, the significant higher Hg content of the floodplain soils was the main factor resulting in the vastly elevated Hg flux from soils compared with BFS/BOFS.

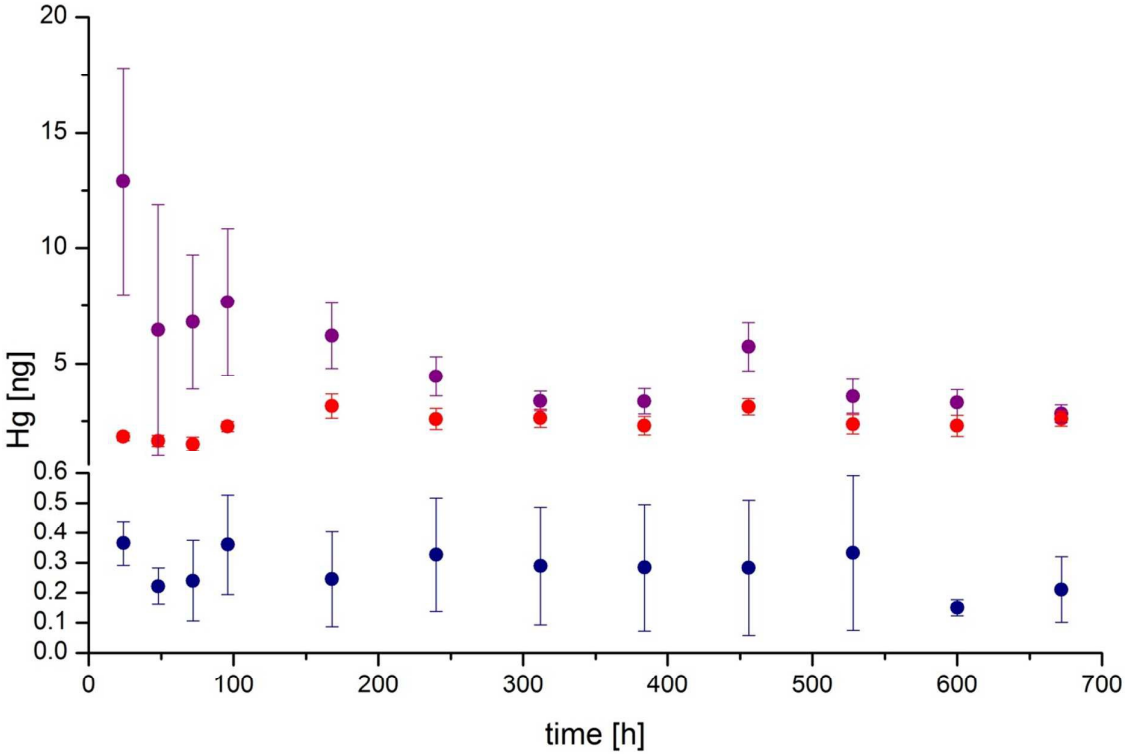

Fig. 3: Averaged vapor phase Hg release from the columns at different temperatures (blue, 15 °C; purple, 25 °C; red, 35 °C). Note the different scale at the y-axis. Error bars were calculated from four replications.

Mercury flux at 35 °C showed similar trends as observed for 15 and 25° C: Hg release was 1.82 ± 0.330 ng ($\bar{x}_m$: 1.75 ng) per 24 h within 100 h and decreased thereafter being 2.64 ± 0.337 ng (($\bar{x}_m$: 2.60 ng) per 72 h. Mercury flux was below the saturation concentration of 43 µg L^{-1}. Surprisingly, the Hg fluxes at 35 °C were significantly lower than at 25 °C. Various research groups have confirmed that temperature favored Hg desorption from soils due to the increase in Hg vapor pressure with increasing temperature. Gillis and Miller[33] showed that Hg emissions in low-Hg, fine sandy loam soils could be largely explained by variations in surface soil temperature and the Hg concentration gradient between the soil and the ambient air. This temperature dependence had also been observed in both diurnal[32] and seasonal studies[34]. Choi and Holsen[17] investigated the impact of solar radiation and soil surface temperature on Hg emissions fluxes using, among others, native deciduous soils (DS) and sterilized deciduous soils (SDS). Experiments conducted in the dark gave high correlations with Hg emissions from both DS and SDS. The average Hg emissions increased from 10 ng m^{-2} h^{-1} at 25 °C to 120 ng m^{-2} h^{-1} at 35 °C for DS and from < 5 ng m^{-2} h^{-1} at 23 °C to 15 ng m^{-2} h^{-1} at 30 °C for SDS. They assumed that the differences between emissions from DS and SDS at the same temperature resulted from differences in biological Hg reduction, mediated by soil microbes. However, this is in contrast with our finding of 25 and 35 °C temperature variants. An explanation of the decreasing Hg flux with increasing temperature from 25 to 35 °C in our experiments might be the water content of the BFS/BOFS sample. Pannu et al.[35] comprehensively summarized the effect of varying

water-filled pore space (WFPS) on soil respiration, indicating that a soil water content equivalent to 60 % of a soil's water holding capacity delineated the point of maximum aerobic microbial activity. In their study, they found that the maximum mass of cumulative Hg^0 was formed at 60 % WFPS and the lowest at 15 % WFPS. Further research reported likewise: Gustin and Stamenkovic[36] observed increased Hg emissions for low-Hg soils with increased water content. A threefold increase in Hg volatilization rate was also described in a field study from November to March (soil moisture increased from 2.8 to 8.4 %) in Hungry Valley, Nevada.[32] Besides bacterial activity, chemical and physical interactions were suggested for enhanced Hg emissions with rising soil moisture: i) physical displacement of Hg^0 enriched interstitial soil air by infiltrating water, (ii) replacement of Hg^0 adsorbed to the soil by water molecules, and (iii) desorption of Hg^{2+} bound to the soil and subsequent reduction to Hg^0 through abiotic or biotic factors.[37] Most likely, BFS/BOFS exhibited vastly limited microbial communities compared to soils, hence biological processes should be inhibited. However, we have no proof for or against biological activity.

Further, it must be stated that column IV at 35 °C had similar water content to all the columns at 25 °C (Table 2) but showed no higher Hg flux; the decreased volatilization rate at 35 °C cannot be solely explained by the water content. At the moment, this phenomenon remains unclear.

As is known for soils and was recently shown by Wang et al.[38] for baghouse filter dust (BFD), Hg emissions from surface material were affected by the Hg content in the upper few centimeters and hence by the air exchange surface area. Extrapolating volatilization from the columns' diameter yielded total Hg emissions of roughly 500 ng per m^2 and 4 weeks for 25 °C. Assuming a linear correlation between total Hg and the volatilization rate from BFS/BOFS (0.25 % within 4 weeks at 25 °C), this would have led to Hg flux of 0.410 µg per m^2 and 4 weeks ($\bar{x}_m$ Hg content of BFS:

1.64 mg kg^{-1}) and to Hg flux of 5.2 mg per m^2 and 4 weeks (max. Hg content of BFS: 20.8 mg kg^{-1}) for the previously studied BFS.[12]

However, transferring this data to other BFS or BFS/BOFS samples can be done only with caution. As Huggins et al.[39] have shown by X-ray absorbance spectroscopy, Hg formed a variety of surface species on unburned C. Thus, differences in C levels of the charge material may affect the speciation of Hg and hence the release of these species.

Furthermore, it must be stated that various research groups have shown that a significant proportion of gaseous Hg from industrial locations may comprise oxidized Hg, such as $HgBr_2$ and $HgCl_2$. Wang et al.[40] recently studied Hg emissions in flue gases of three cement plants in China, showing that oxidized Hg was the major species of total Hg in flue gas (61 to 91 %). Moreover, Wang et al.[38] determined Hg concentration and speciation in BFD from a cement kiln in the State of Florida. They found that the concentration of oxidized Hg ranged between 62 and 73 %. Also, in coal-fired flue gas, oxidized Hg species have a significant presence. The fraction of oxidized Hg in the flue gas of a particular power plant largely depends on the coal type, combustion efficiency, and the pollution control equipment used. However, as oxidized Hg species are water soluble and the BFS/BOFS had already passed a wet cleaning process, most of these species should already be removed. Hence, volatilization of oxidized Hg from BFS/BOFS should be significantly lower or below the detection limit.

4. Conclusions

Blast furnace sludge mixed with BOFS contained a significant amount of Hg. Volatilization of Hg from BFS/BOFS was proved for the first time. Despite rather low volatilization of Hg from fresh BFS/BOFS for all temperature ranges, emissions of Hg

to the atmosphere are of environmental concern due to its long atmospheric lifetime and the bioaccumulation after deposition. However, in countries with less strict environmental laws, pure BFS or BFS/BOFS with significantly higher Hg content may be used in landfill and hence vastly contribute to the global Hg cycle via volatilization. As only elemental Hg vapor was determined in this study, but as oxidized Hg species may be present as well, experiments quantifying these species (e.g. with potassium chloride denuders) also should be conducted to quantify the environmental exposure by volatilization from BFS and/or BOFS. Further, the potential sunlight driven reduction of oxidized Hg to elemental Hg should be studied, as this may influence Hg emissions.

1. P. Van Herck, C. Vandecasteele, R. Swennen and R. Mortier, *Environ. Sci. Technol.*, 2000, **34**, 3802-3808.
2. T. Mansfeldt and R. Dohrmann, *Environ. Sci. Technol.*, 2004, **38**, 5977-5984.
3. Z. H. Trung, F. Kukurugya, Z. Takacova, D. Orac, M. Laubertova, A. Miskufova and T. Havlik, *J. Hazard. Mater.*, 2011, **192**, 1100-1107.
4. K. Gargul and B. Boryczko, *Archives of Civil and Mechanical Engineering*, 2015, **15**, 179-187.
5. B. Das, S. Prakash, P. S. R. Reddy and V. N. Misra, *Resour. Conserv. Recy.*, 2007, **50**, 40-57.
6. H. T. Makkonen, J. Heino, L. Laitila, A. Hiltunen, E. Poylio and J. Harkki, *Resour. Conserv. Recy.*, 2002, **35**, 77-84.
7. S. Hyoung-Ky, M. Seok-Min and J. Jin-Nam, Recycling of waste materials for iron ore sintering, The United Nations Economic Commission for Europe, Düsseldorf, 1995.
8. World Steel Association, Crude steel production, Retrieved from http://www.worldsteel.org/dms/internetDocumentList/statistics-archive/production-archive/steel-archive/steel-annually/steel-annually-1980-2013/document/steel%20annually%201980-2013.pdf.
9. A. Lopez-Delgado, C. Perez and F. A. Lopez, *Water Res.*, 1998, **32**, 989-996.
10. World Steel Association, World Steel in Figures 2014, Retrieved from http://www.worldsteel.org/dms/internetDocumentList/bookshop/World-Steel-in-Figures-2014/document/World%20Steel%20in%20Figures%202014%20Final.pdf.
11. M. V. Cantarino, Master of Science Thesis, Universidade Federal de Minas Gerais, 2011.
12. C. Foeldi, R. Dohrmann and T. Mansfeldt, *Chemosphere*, 2014, **99**, 248-253.
13. WHO, Mercury in drinking-water. Background document for develoment of WHO Guidelines for drinking-water quality, World Health Organisation (WHO/SDE/WSH/05.08/10), Geneva, 2005.
14. UNEP, *Global Mercury Assessment 2013, Sources, Emissions, Releases and Environmental Transport*, UNEP Chemicals Branch, Geneva, 2013.
15. K. Schlüter, *Environ. Geol.*, 2000, **39**, 249-271.
16. Å. Iverfeldt, Doctor of Philosophy, University of Göteborg, 1984.
17. H.-D. Choi and T. M. Holsen, *Environ. Pollut.*, 2009, **157**, 1673-1678.
18. S. E. Lindberg, G. R. Southworth, M. A. Bogle, T. J. Blasing, J. Owens, K. Roy, H. Zhang, T. Kuiken, J. Price, D. Reinhart and H. Sfeir, *J. Air Waste Manage.*, 2005, **55**, 859-869.

19. G. R. Southworth, S. E. Lindberg, M. A. Bogle, H. Zhang, T. Kuiken, J. Price, D. Reinhart and H. Sfeir, *J. Air Waste Manage.*, 2005, **55**, 870-877.
20. Z. G. Li, X. Feng, P. Li, L. Liang, S. L. Tang, S. F. Wang, X. W. Fu, G. L. Qiu and L. H. Shang, *Atmos. Chem. Phys.*, 2010, **10**, 3353-3364.
21. M. Gustin and D. Jaffe, *Environ. Sci. Technol.,* 2010, **44**, 2222-2227.
22. J. Rinklebe, A. During, M. Overesch, R. Wennrich, H.-J. Staerk, S. Mothes and H.-U. Neue, *Ecol. Eng.*, 2009, **35**, 319-328.
23. NOAA National Climatic Data Center, State of the Climate: Global Analysis for Annual 2014, Retrieved from http://www.ncdc.noaa.gov/sotc/global/201413.
24. R. Kretzschmar, T. Mansfeldt, P. N. Mandaliev, K. Barmettler, M. A. Marcus and A. Voegelin, *Environ. Sci. Technol.*, 2012, **46**, 12381-12390.
25. J. Veres, S. Jakabsky and V. Sepelak, *Diffus. Fundam.*, 2010, **12**, 88-91.
26. J. Veres, S. Jakabsky and M. Lovas, *Acta Montan. Slovaca*, 2011, **16**, 185-191.
27. H. Nogami, J.-i. Yagi, S.-y. Kitamura and P. R. Austin, *Isij Int.*, 2006, **46**, 1759-1766.
28. P. S. Hooda, *Trace Elemnts in Soils*, John Wiley & Sons Ltd, West Sussex, 2010.
29. J. Veres, M. Lovas, S. Jakabsky, V. Sepelak and S. Hredzak, *Hydrometallurgy*, 2012, **129**, 67-73.
30. Occupational Safety & Health Administration, *Mercury Vapor In Workplace Atmospheres*, United States Department of Labor, Washington, DC, 2010.
31. I. Hindersmann, J. Hippler, A. V. Hirner and T. Mansfeldt, *J.Soil. Sediment.*, 2014, **14**, 1549-1558.
32. M. S. Gustin, M. Engle, J. Ericksen, S. Lyman, J. Stamenkovic and M. Xin, *Appl. Geochem.*, 2006, **21**, 1913-1923.
33. A. A. Gillis and D. R. Miller, *Sci. Total Environ.*, 2000, **260**, 191-200.
34. J. M. Sigler and X. Lee, *J. Geophys. Res.: Biogeo.*, 2006, **111**.
35. R. Pannu, S. D. Siciliano and N. J. O'Driscoll, *Environ. Pollut.*, 2014, **193**, 138-146.
36. M. S. Gustin and J. Stamenkovic, *Biogeochemistry*, 2005, **76**, 215-232.
37. S. E. Lindberg, H. Zhang, M. Gustin, A. Vette, F. Marsik, J. Owens, A. Casimir, R. Ebinghaus, G. Edwards, C. Fitzgerald, J. Kemp, H. H. Kock, J. London, M. Majewski, L. Poissant, M. Pilote, P. Rasmussen, F. Schaedlich, D. Schneeberger, J. Sommar, R. Turner, D. Wallschlager and Z. Xiao, *J. Geophys. Res.: Atmos.*, 1999, **104**, 21879-21888.
38. J. Wang, J. Hayes, C.-Y. Wu, T. Townsend, J. Schert, T. Vinson, K. Deliz and J.-C. Bonzongo, *Environ. Sci. Technol.*, 2014, **48**, 2481-2487.
39. F. E. Huggins, N. Yap, G. P. Huffman and C. L. Senior, *Proc. Air Waste Manage. Assoc. Meet., 92 Annual Meeting,Pittsburgh, PA, June 20-24, 1999; pp 2116-2127.*, 1999.
40. F. Wang, S. Wang, L. Zhang, H. Yang, Q. Wu and J. Hao, *Atmos. Environ.*, 2014, **92**, 421-428.

Mercury (Hg) is considered as one of the most important environmental pollutants, as the element and many of its compounds are highly toxic and bioaccumulative. Blast furnace sludge (BFS) is an industrial waste with elevated Hg contents due to enrichment during the production process of pig iron. This study is the first to analyze Hg volatilization from BFS and the effect of temperature on Hg fluxes. The results are of significant implications as this waste has long been dumped in large surface landfills in Europe, which might be an ongoing procedure in countries with less strict environmental laws. Hence, volatilization potential of Hg from this waste is of special environmental concern.